DETACHED EDDY SIMULATIONS: ANALYSIS OF A LIMIT ON THE DISSIPATION TERM FOR REDUCING SPECTRAL ENERGY TRANSFER AT CUT-OFF

L. Davidson[1], *C. Friess*[2]

[1] ***Div. of Fluid Dynamics***
Dept. of Mechanics and Maritime Sciences (M2)
Chalmers University of Technology, Gothenburg, Sweden
[2] ***Aix-Marseille Université, CNRS, Centrale Marseille***
M2P2 UMR 7340, 13451, Marseille, France

lada@chalmers.se

Abstract

In Detached Eddy Simulations (DES[1] and ID-DES [2]), part of the flow is URANS mode (where most of the turbulence is modeled by a RANS model) and the other part is in LES mode (where most of the turbulence is resolved). Between these regions the partition of turbulent kinetic between URANS mode and LES mode changes seamlessly (as in IDDES) or somewhat more abruptly (as in DES). Looking at the energy spectrum this change of partition can be seen as a change of the cut-off wavenumber, κ_c. In this paper we formulate a limitation – based on perturbation analysis – on how to reduce the spatial change in partition. This is achieved simply by setting a limit on the dissipation term in the k equation in the LES region. This slows down the spatial transition from RANS to LES at RANS-LES interfaces in boundary layers, embedded LES and – depending of boundary condition on k – at inlets. It is found to give at least as good results as the standard IDDES model. For the hump flow, the IDDES-PC model gives better results than the IDDES model.

1 Introduction

In [3] they performed perturbation analyses about the equilibrium states, representing small variation of the turbulent kinetic energy partition. The analysis was performed along a streamline assuming that the left-hand sides of the k and ε equations are zero. They introduced a H-equivalence between PITM/PANS[4, 5] and DES. Later on, new formulations of the PANS model were presented mimicking the DES model [6] and the IDDES model [7]. The two new PANS models were denoted D-PANS and ID-PANS, respectively. In [7] it was found that the ID-PANS model was numerically more stable than its parent IDDES model. A smaller time step had to be used in IDDES than in

ID-PANS.

In the present work we propose how to limit the spatial change of partition between resolved and modeled turbulence. We will, furthermore, extend the perturbation analysis to flows where we include the left-hand side of the k and ε equations neglecting the diffusion term. We denote the new model IDDES-PC (Partition Control).

2 The turbulence models

The low-Reynolds number for IDDES and PITM (Partially Integrated Transport Modeling) reads

$$
\begin{aligned}
\frac{\partial k}{\partial t} + \frac{\partial \bar{u}_j k}{\partial x_j} &= \frac{\partial}{\partial x_j}\left[\left(\nu + \frac{\nu_t}{\sigma_k}\right)\frac{\partial k}{\partial x_j}\right] + P_k - \psi\varepsilon \\
\frac{\partial \varepsilon}{\partial t} + \frac{\partial \bar{u}_j \varepsilon}{\partial x_j} &= \frac{\partial}{\partial x_j}\left[\left(\nu + \frac{\nu_t}{\sigma_\varepsilon}\right)\frac{\partial \varepsilon}{\partial x_j}\right] + C_{\varepsilon 1} f_1 P_k \frac{\varepsilon}{k} - C_{\varepsilon 2}^* \frac{\varepsilon^2}{k} \\
C_{\varepsilon 1} &= 1.5, \quad C_{\varepsilon 2} = 1.9, \quad C_\mu = 0.09 \\
\nu_t &= C_\mu f_\mu \frac{k^2}{\varepsilon}, \quad \sigma_k = 1.4, \quad \sigma_\varepsilon = 1.4
\end{aligned}
\tag{1}
$$

where the damping functions are defined as

$$
\begin{aligned}
f_2 &= \left[1 - \exp\left(-\frac{y^*}{3.1}\right)\right]^2\left\{1 - 0.3\exp\left[-\left(\frac{R_t}{6.5}\right)^2\right]\right\} \\
f_\mu &= \left[1 - \exp\left(-\frac{y^*}{14}\right)\right]^2\left\{1 + \frac{5}{R_t^{3/4}}\exp\left[-\left(\frac{R_t}{200}\right)^2\right]\right\}
\end{aligned}
$$

PITM

The coefficient in the ε equation reads $C_{\varepsilon 2}^* = C_{\varepsilon 1} + f_k(C_{\varepsilon 2}f_2 - C_{\varepsilon 1})$ and $\psi = 1$. The function f_k is computed based on IDDES/DES and the equivalence criterion [7]

$$
f_k = \min\left\{1, \max\left[\frac{C_{\varepsilon 2} - C_{\varepsilon 1}\psi}{C_{\varepsilon 2} - C_{\varepsilon 1}}, 0\right]\right\}
\tag{2}
$$

The PITM model is used in the analysis below. It is not included in the results section.
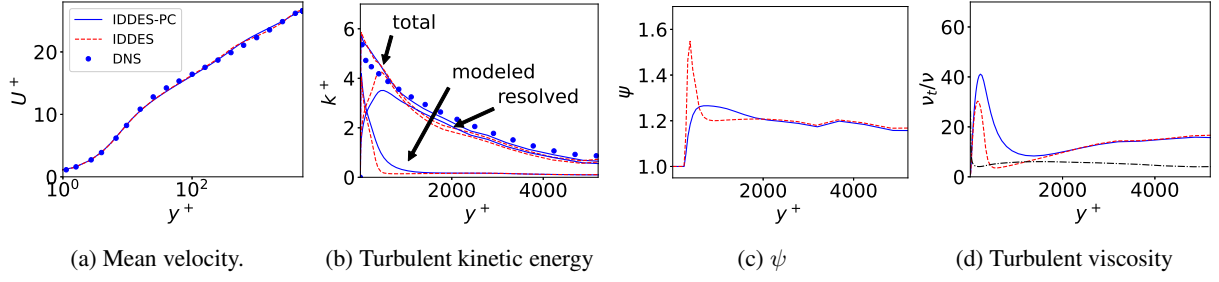
Figure 1: Channel flow, periodic boundary conditions. ——— : IDDES-PC model; ━ ━ : IDDES; ━ · ━ : Smagorinsky model using the IDDES-PC velocity field; Markers: DNS [8]

IDDES and IDDES-PC

The coefficient in the ε equation is constant, $C_{\varepsilon 2}^* = C_{\varepsilon 2}$ and ψ in the k equation is computed as

$$\psi = \max\left(1, \frac{k^{3/2}/\varepsilon}{L_{IDDES}}\right)$$

where L_{IDDES} is the usual IDDES length scale [2, 7]

$$L_{IDDES} = f_d(1 + f_e)\frac{k^{3/2}}{\varepsilon} + (1 - f_d)C_{DES}\Delta$$

IDDES-PC differs from IDDES by the use of a limiter for ψ, which is derived below.

3 Analysis

Let us define the modeled ensemble-averaged k and ε, i.e. $k_M = \langle k \rangle$ and $\varepsilon_M = \langle \varepsilon \rangle$. Along mean streamlines, k_M and ε_M are assumed to be in equilibrium, which yields, when describing both PITM and IDDES

$$\frac{dk_M}{dt} = P^k + D^k - \psi\varepsilon_M = 0 \quad (3)$$

$$\frac{d\varepsilon_M}{dt} = C_{\varepsilon 1}\frac{\varepsilon_M}{k_M}P^k + D^\varepsilon - C_{\varepsilon 2}^*\frac{\varepsilon_M^2}{k_M} = 0 \quad (4)$$

$$\psi = \max\left(1, \frac{k^{3/2}/\varepsilon}{C_{DES}\Delta_{max}}\right) \quad (5)$$

We introduce a perturbation, δk_M, which slightly moves the cut-off between resolved and modeled scales. We assume that does not affect the dissipation, i.e

$$\delta\varepsilon_M = 0. \quad (6)$$

Following [3], we assume that $\delta k_M/k_M$ does not vary in space, i.e.

$$\frac{\partial(\delta k_M/k_M)}{\partial x_j} = 0 \Rightarrow \frac{1}{k_M}\frac{\partial(\delta k_M)}{\partial x_j} - \frac{\delta k_M}{k_M^2}\frac{\partial k_M}{\partial x_j} = 0$$

which gives

$$\frac{\partial(\delta k_M)}{\partial x_j} = \frac{\delta k_M}{k_M}\frac{\partial k_M}{\partial x_j} \quad (7)$$

The relation above implies that the spatial change of partition between resolved and modeled turbulence is

proportional to that of the modeled turbulence; this is a physical, reasonable assumption.

For the PITM model, the perturbation analysis gives [7, 9]

$$\delta C_{\varepsilon 2}^* = \frac{3\delta k_M}{k_M}(C_{\varepsilon 2}^* - C_{\varepsilon 1}) \Rightarrow \frac{\delta f_k}{f_k} = \frac{3\delta k_M}{k_M} \quad (8)$$

We find – as expected – that there is a linear relation between a change in the turbulence kinetic energy partition, δk_M, and f_k. When f_k increases (i.e. the cut-off wavenumber moves to a lower wavenumber), then δk_M increases (i.e. more turbulence is modeled).

For the IDDES/DES model, the equations for infinitesimal perturbations of Eqs. 3-4 are

$$\delta P^k + \delta D^k - \varepsilon_M\delta\psi = 0$$

$$C_{\varepsilon 1}\frac{\varepsilon_M}{k_M}P^k\left(\frac{\delta P^k}{P^k} - \frac{\delta k_M}{k_M}\right)$$

$$+C_{\varepsilon 2}\frac{\varepsilon_M^2}{k_M}\left(\frac{\delta k_M}{k_M}\right) + \delta D^\varepsilon = 0$$

The perturbation analysis gives [7, 9]

$$\delta\psi = \frac{3(C_{\varepsilon 1}\psi - C_{\varepsilon 2})}{C_{\varepsilon 1}}\frac{\delta k_M}{k_M} \Rightarrow$$

$$\frac{\delta\psi}{\psi} = \frac{3\delta k_M}{k_M}\left(1 - \frac{C_{\varepsilon 2}}{C_{\varepsilon 1}\psi}\right) \quad (9)$$

For $\psi < C_{\varepsilon 2}/C_{\varepsilon 1}$, the relation is as expected: an increase in ψ – due to, for example, a decrease in Δ_{max} – corresponds to a negative δk_M (i.e. less modeled and more resolved turbulence). But for $\psi > C_{\varepsilon 2}/C_{\varepsilon 1}$ this relation is reversed. The reason is probably that Eq. 7 is not valid. One way to make sure that Eq. 7 is not violated is to introduce a limit on ψ as

$$\psi \le C_{\varepsilon 2}/C_{\varepsilon 1} \quad (10)$$

In this way we get a modified IDDES model – denoted IDDES-PC (Partition Control)– in which the change in turbulence kinetic energy partition obeys Eq. 7.

Above we made an analysis neglecting the convection terms while retaining the diffusion terms, see Eq. 3. Next, we make an assumption that the diffusion term is negligible but we retain the convection term,

C^k, i.e.

$$P^k - C^k - \psi\varepsilon_M = 0$$
$$C_{\varepsilon 1}\frac{\varepsilon_M}{k_M}P^k - C^\varepsilon - C_{\varepsilon 2}^*\frac{\varepsilon_M^2}{k_M} = 0$$

A perturbation analysis gives, using Eq. 7, for the PITM model [9]

$$\frac{\delta f_k}{f_k} = \frac{\delta k_M}{k_M} \qquad (11)$$

and for the IDDES/DES model [9]

$$\frac{\delta\psi}{\psi} = \frac{\delta k_M}{k_M}\left(1 - \frac{C_{\varepsilon 2}}{C_{\varepsilon 1}\psi}\right) \qquad (12)$$

The limit on ψ for the IDDES/DES model when accounting for convection is the same as when accounting for diffusion (see Eq. 9).

The perturbation analysis presented above – both when neglecting the diffusion and the convection – gives the same limit on ψ, i.e. Eq. 10. This limit is expected to be active when the spatial gradients of the turbulence kinetic energy partition –and the gradient of k itself – is largest, i.e. in regions where the changes in cut-off wavenumber, κ_c, is strongest. We expect this to happen at RANS-LES interface in a boundary layer, at embedded RANS-LES interface and at inlets (provided that the inlet boundary conditions for k are taken from RANS).

4   The numerical method

The finite volume code **pyCALC-LES** [10] is used. It is fully vectorized (i.e. no `for` loops). The solution procedure is based on fractional step. Second-order central differencing is used in space and the Crank-Nicolson scheme in time. For k and ε, the hybrid central/upwind scheme is used together with first-order fully-implicit time discretization. The discretized equations are solved with Pythons sparse matrix solvers. For the pressure Poisson equation, the `pyAMG` solver [11] has been found to be very efficient.

5   Results

The first test case is fully-developed channel flow at $Re_\tau = u_\tau h/\nu = 5\,200$, where h denotes half-channel width. The size of the domain is $x_{max} = 3.2$, $y_{max} = 2$ and $z_{max} = 1.6$. The mesh has $32 \times 96 \times 32$ (x, y, z) cells which gives $(\Delta x^+, \Delta z^+) = (800, 400)$.

Figure 1a shows that both models give virtually the same velocity profiles. The strongest change in partition between modeled and resolved turbulence – due to turbulent diffusion – occurs in the interface region between RANS and LES. The theoretical maximum partition change is given by Eq. 9. It can be seen in Fig. 1b that when going from RANS to LES the modeled turbulence decreases faster – i.e. the energy partition changes faster – for the IDDES model compared

to IDDES-PC. The reason is – of course – that we limit the change in turbulence kinetic energy partition in the IDDES-PC model. Figure 1c shows ψ and we see that the limitation in ψ in the IDDES-PC model takes place in the LES region close to the RANS-LES interface. The turbulent viscosity (Fig. 1d) predicted by the IDDES-PC in the LES region near the interface does not exhibit any local minimum near the RANS-LES interface as does the IDDES model. The first impression may be that the IDDES-PC does not sufficiently reduce the turbulent viscosity in the LES region near the RANS-LES interface. But on the other hand, why should the turbulent viscosity in the LES region close to the RANS-LES interface exhibit a local minimum as does the IDDES model? The Smagorinsky model gives a peak in the turbulent viscosity at the same location (the Smagorinsky turbulent viscosity is computed for post-processing in the IDDES-PC simulation) as the location of the minimum with the IDDES model. Finally, it should be noted that many DES/PANS models predict a local minimum in turbulent viscosity near the interface, see e.g. [12].

The second test case is channel flow with inlet-outlet. The same mesh is used as above in the y and z directions. In the x direction, the extent is $x_{max} = 9$ using 96 cells. The inlet k is taken from a 1D RANS. Following Eq. 6, Neumann is used for ε, i.e. $\partial\varepsilon/\partial x = 0$. The object is to study how fast the turbulence models change the partition from modeled to resolved turbulence when going from RANS to LES near the inlet. The theoretical partition change is given by Eq. 12. Figure 2a shows that both models give reasonable good results (including commutation terms improves the result, see below, but it is not such a good test case for partition change). The modeled, turbulent kinetic energy in Fig. 2b shows the same trend as for fully-developed channel flow: the change in partition is much faster for IDDES than for IDDES-PC.

The third test is identical to the second, except that we in the k equation add a commutation term including $\partial f_k/\partial x$ at the plane adjacent to the inlet. The object is to reduce the inlet k, prescribed from 1D RANS, where f_k is taken from the equivalence criterion in Eq. 2; $f_k = 1$ at the inlet. The commutation term reads (Interface Model 2 in [12]).

$$P_c = k_{tot}\bar{u}_1\frac{\partial f_k}{\partial x} \qquad (13)$$

where k_{tot} is the sum of resolved (running average) and modeled turbulent kinetic energy. For more detail on inlet synthetic fluctuations and the commutation term, see [12].

Figure 3 presents the friction velocity, the modeled k, ψ and the turbulent viscosity. Thanks to the commutation term, the modeled turbulent kinetic energy is quickly reduced from RANS values at the inlet to appropriate LES values. The ψ function is limited in the entire LES region. Far downstream (not shown), the limit is active only near the RANS-LES interface
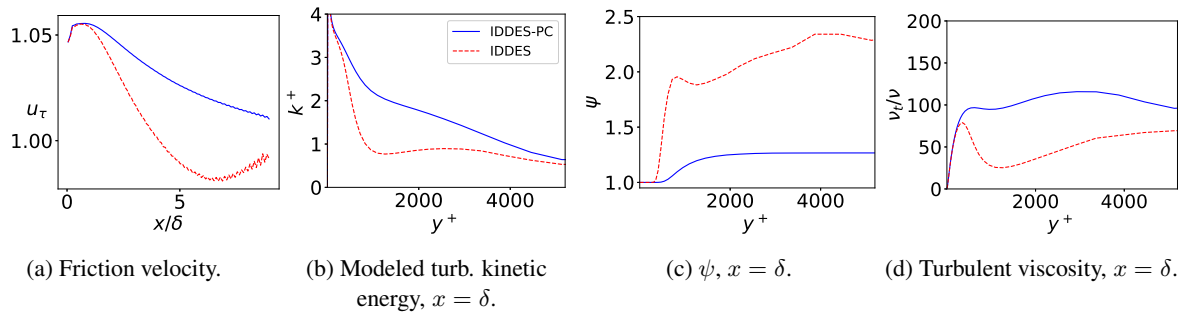
(a) Friction velocity.

(b) Modeled turb. kinetic
energy, $x = \delta$.

(c) ψ, $x = \delta$.

(d) Turbulent viscosity, $x = \delta$.

Figure 2: Channel flow, inlet-outlet without commutation term at the inlet. δ denote half-channel width.

(a) Friction velocity.

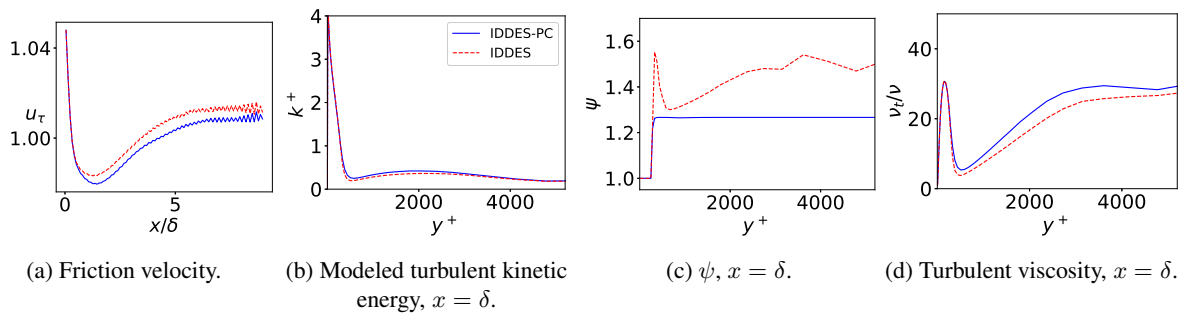(b) Modeled turbulent kinetic
energy, $x = \delta$.

(c) ψ, $x = \delta$.

(d) Turbulent viscosity, $x = \delta$.

Figure 3: Channel flow, inlet-outlet with commutation term at the inlet. Markers: DNS [8]

(a) Grid. Every 6th grid line.

(b) Pressure coefficient.

(c) Skin friction
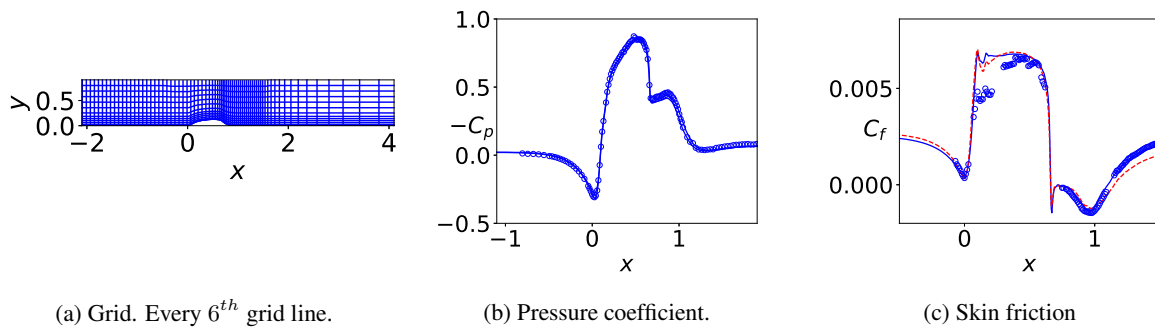
Figure 4: Hump flow. ——— : IDDES-PC model; — — . IDDES. Markers: experiments [13, 14]

(a) $x = 0.65$.

(b) $x = 1.0$.

(c) $x = 1.30$.
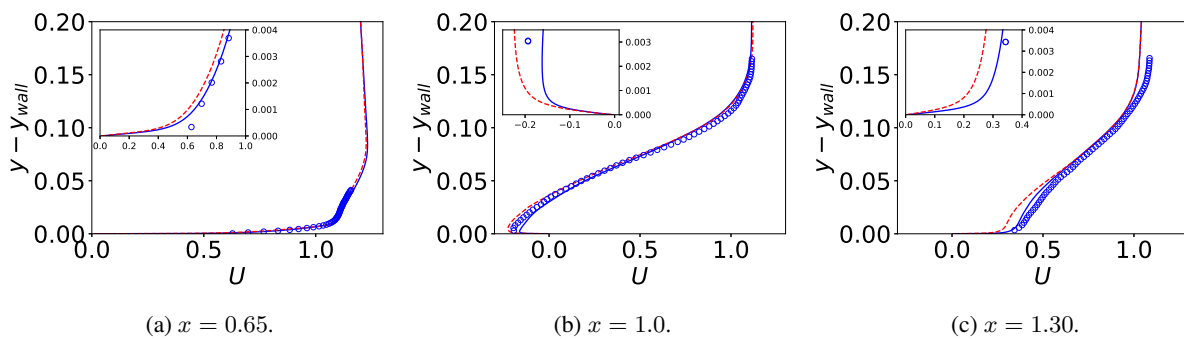
Figure 5: Hump flow. Velocities. ——— : IDDES-PC model; — — . IDDES. Markers: experiments [13, 14]
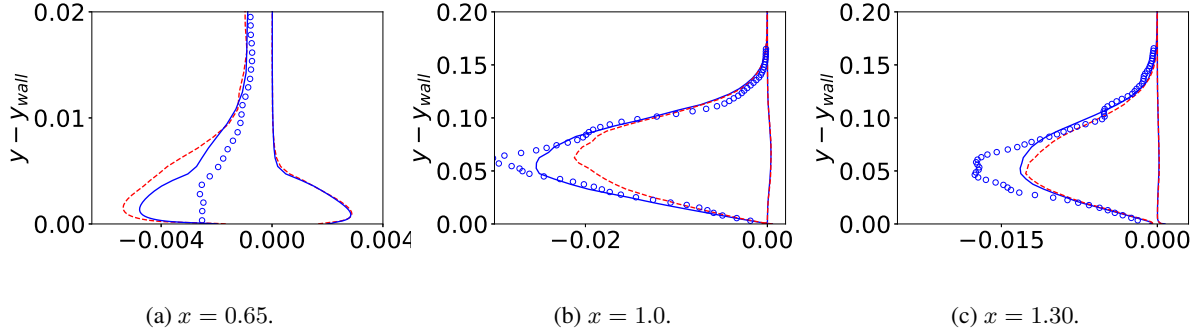
(a) $x = 0.65$.   (b) $x = 1.0$.   (c) $x = 1.30$.

Figure 6: Hump flow. Total and (minus) modeled shear stresses. ——— : IDDES-PC model; – – . IDDES. Markers: experiments [13, 14]

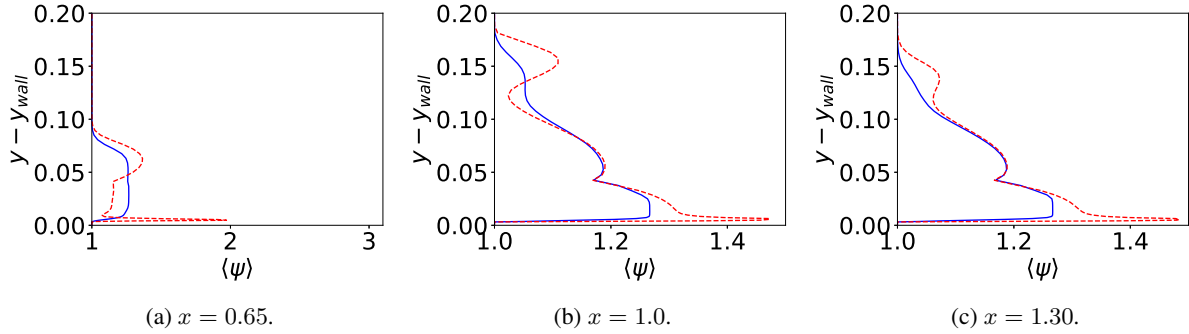(a) $x = 0.65$.   (b) $x = 1.0$.   (c) $x = 1.30$.

Figure 7: Hump flow. ψ. ——— : IDDES-PC model; – – . IDDES. Markers: experiments [13, 14]

(a) Streamwise fluctuations. $x = 0$
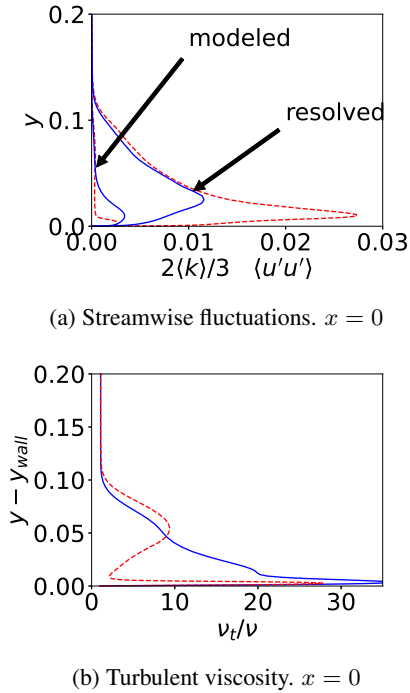

(b) Turbulent viscosity. $x = 0$

Figure 8: Hump flow. ——— : IDDES-PC model; – – . IDDES.

(as in Fig. 1c). It may be noted – contrary to Fig. 1d and 2d – the ψ function exhibits a local minimum in the LES region near the RANS-LES interface also for the IDDES-PC model. The reason is the commutation term in Eq. 13 which is large in the interface region (k_{tot} is large).

The fourth test case is the flow over a two-dimensional hump. The Reynolds number of the hump flow is $Re_c = 936\,000$, based on the hump length, $c = 1$, and the inlet mean velocity at the centerline, $U_{in,c} = 1$. The time step is set to $0.003c/U_{in,c}$. The inlet is located at $x = -2.1$ and the outlet at $x = 4.0$. The spanwise extent is $z_{max} = 0.2$. The mesh has $582 \times 128 \times 32$ cells (x, y, z) and it is based on the mesh in [15] but it is refined in the region $-2.1 \le x \le -1$ so that $\Delta x = 0.01$ for $x < 0$, see Fig. 4a. The inlet mean flow and the turbulent quantity, k is set from a 2D RANS simulation and $\partial \varepsilon / \partial x = 0$. Anisotropic fluctuations are superimposed on the mean flow in the same way as in the channel flow simulation and the commutation term in Eq. 13 is employed.

Figures 4b and 4c compare predicted pressure coefficient and skin friction with experiment. The agreement is good for both models. The IDDES model gives slightly too strong a recirculation region which is seen also in the velocity profiles (Fig. 5). The total shear stress and the modeled shear stress are presented in Fig. 6 (to enhance visibility, the negative modeled shear stresses are plotted). Both models over-predict the magnitude of the shear stress at $x = 0.65$. This

was also seen in [7, 15]. Figure 7 presents ψ and it is seen that the limit of ψ in the IDDES-PC is active in a large region in the attached boundary at $x = 0.65$ but further downstream it is active up to approximately $y - y_{wall} < 0.02$. For the IDDES model, ψ has at $x = 0.65$ a local peak at $y - y_{wall} \simeq 0.07$ which further downstream moves away from the wall. The peak has probably its origin at $x = 0$ where the IDDES model predicts a large peak in $\langle u'u' \rangle$, see Fig. 8a. This peak is almost three times larger than the peak in the experiments at $x = 0.65$ (not shown). Figure 8b shows the turbulent viscosity and it can be seen that the IDDES gives a local peak at $x \simeq 0.07$ (the same location as ψ). Such a minimum in the turbulent viscosity in the LES region close to the RANS-LES interface was also seen in the channel flows (Figs. 1d and 2d).

6 Conclusions

A new limit on spatial gradient of partition between modeled and resolved turbulent kinetic energy is presented. Looking at the turbulent kinetic energy spectrum, the location of partition corresponds to the cut-off wavenumber, κ_c. The limit was introduced in the perturbation analyses in [3]. It states that the spatial gradient of κ_c is related to that of k.

It is found that the new model does reduce the gradient of κ_c in the RANS-LES interface regions as it should. It is found to give at least as good results as the standard IDDES model. For the hump flow, the IDDES-PC model gives better results than the IDDES model. The reason may be that the resolution in the boundary layer approaching the hump is too low or that the synthetic fluctuations are not good enough. This issue will be addressed in the near future using a refined mesh and inlet boundary conditions from a pre-cursor simulation.

The new limit is in this work used in the IDDES model. It could probably be used in any DES model.

Acknowledgments

References

[1] P. R. Spalart, W.-H. Jou, M. Strelets, and S. R. Allmaras. Comments on the feasability of LES for wings and on a hybrid RANS/LES approach. In C. Liu and Z. Liu, editors, *Advances in LES/DNS, First Int. conf. on DNS/LES*, Louisiana Tech University, 1997. Greyden Press.

[2] M. L. Shur, P. R. Spalart, M. Kh. Strelets, and A. K. Travin. A hybrid RANS-LES approach with delayed-DES and wall-modelled LES capabilities. *International Journal of Heat and Fluid Flow*, 29:1638–1649, 2008. URL https://doi.org/10.1016/j.ijheatfluidflow.2008.07.001.

[3] Ch. Friess, R. Manceau, and T.B. Gatski. Toward an equivalence criterion for hybrid RANS/LES methods. *International Journal of Heat and Fluid Flow*, 122:233–246, 2015. URL https://doi.org/10.1016/j.compfluid.2015.08.010.

[4] R. Schiestel and A. Dejoan. Towards a new partially integrated transport model for coarse grid and unsteady turbulent flow simulations. *Theoretical and Computational Fluid Dynamics*, 18(6):443–468, 2005. URL https://doi.org/10.1007/s00162-004-0155-z.

[5] S. S. Girimaji. Partially-averaged Navier-Stokes model for turbulence: A Reynolds-averaged Navier-Stokes to direct numerical simulation bridging method. *ASME Journal of Applied Mechanics*, 73(2):413–421, 2006. URL https://doi.org/10.1115/1.2151207.

[6] L. Davidson and C. Friess. A new formulation of f_k for the PANS model. *Journal of Turbulence*, pages 1–15, 2019. doi: 10.1080/14685248.2019.1641605. URL http://dx.doi.org/10.1080/14685248.2019.1641605.

[7] C. Friess and L. Davidson. A formulation of PANS able to mimic IDDES. *International Journal of Heat and Fluid Flow*, 86(108666), 2020. URL https://doi.org/10.1016/j.ijheatfluidflow.2020.108666.

[8] M. Lee and R. D. Moser. Direct numerical simulation of turbulent channel flow up to $Re_\tau \approx 5200$. *Journal of Fluid Mechanics*, 774:395–415, 2015. doi: 10.1017/jfm.2015.268. URL https://doi.org/10.1017/jfm.2015.268.

[9] L. Davidson. Fluid mechanics, turbulent flow and turbulence modeling. eBook, Division of Fluid Dynamics, Dept. of Mechanics and Maritime Sciences, Chalmers University of Technology, Gothenburg, 2014.

[10] L. Davidson. pyCALC-LES: a Python code for DNS, LES and Hybrid LES-RANS. Division of Fluid Dynamics, Dept. of Mechanics and Maritime Sciences, Chalmers University of Technology, Gothenburg, 2021.

[11] L. N. Olson and J. B. Schroder. PyAMG: Algebraic multigrid solvers in Python v4.0, 2018. URL https://github.com/pyamg/pyamg.

[12] L. Davidson. Zonal PANS: evaluation of different treatments of the RANS-LES interface. *Journal of Turbulence*, 17(3):274–307, 2016. URL http://dx.doi.org/10.1080/14685248.2015.1093637.

[13] D. Greenblatt, K. B. Paschal, C.-S. Yao, J. Harris, N. W. Schaeffler, and A. E. Washburn. A separation control CFD validation test case. Part 1: Baseline & steady suction. AIAA-2004-2220, 2004.

[14] D. Greenblatt, K. B. Paschal, C.-S. Yao, and J. Harris. A separation control CFD validation test case Part 1: Zero efflux oscillatory blowing. AIAA-2005-0485, 2005.

[15] A. Garbaruk, E. Guseva, M. Shur, M. Strelets, and A. Travin. 2D wall-mounted hump. In Charles Mockett, Werner Haase, and Dieter Schwamborn, editors, *Go4Hybrid: Grey Area Mitigation for Hybrid RANS-LES Methods*, volume 134 of *Notes on Numerical Fluid Mechanics and Multidisciplinary Design*, pages 173–188. Springer Verlag, 2018.